ELSEVIER

Biochimica et Biophysica Acta 1506 (2001) 117–126

BIOCHIMICA ET BIOPHYSICA ACTA
BBA

www.bba-direct.com

Photosystem II of peas: effects of added divalent cations of Mn, Fe, Mg, and Ca on two kinetic components of P_{680}^+ reduction in Mn-depleted core particles

Ralf Ahlbrink [a], Boris K. Semin [b], Armen Y. Mulkidjanian [a,c], Wolfgang Junge [a,*]

[a] *Division of Biophysics, Department of Biology/Chemistry, University of Osnabrück, 49069 Osnabrück, Germany*
[b] *Chair of Biophysics, Department of Biology, Moscow State University, Moscow 118899, Russia*
[c] *A.N. Belozersky Institute of Physico-Chemical Biology, Moscow State University, Moscow 118899, Russia*

Received 8 March 2001; received in revised form 7 May 2001; accepted 10 May 2001

Abstract

The catalytic Mn cluster of the photosynthetic oxygen-evolving system is oxidized via a tyrosine, Y_Z, by a photooxidized chlorophyll *a* moiety, P_{680}^+. The rapid reduction of P_{680}^+ by Y_Z in nanoseconds requires the intactness of an acid/base cluster around Y_Z with an apparent functional p*K* of <5. The removal of Mn (together with bound Ca) shifts the p*K* of the acid/base cluster from the acid into the neutral pH range. At alkaline pH the electron transfer (ET) from Y_Z to P_{680}^+ is still rapid (<1 μs), whereas at acid pH the ET is much slower (10–100 μs) and steered by proton release. In the intermediate pH domain one observes a mix of these kinetic components (see R. Ahlbrink, M. Haumann, D. Cherepanov, O. Bögershausen, A. Mulkidjanian, W. Junge, Biochemistry 37 (1998)). The overall kinetics of P_{680}^+ reduction by Y_Z in Mn-depleted photosystem II (PS II) has been previously shown to be slowed down by divalent cations (added at >10 μM), namely: Mn^{2+}, Co^{2+}, Ni^{2+}, Cu^{2+}, Zn^{2+} (C.W. Hoganson, P.A. Casey, O. Hansson, Biochim. Biophys. Acta 1057 (1991)). Using Mn-depleted PS II core particles from pea as starting material, we re-investigated this phenomenon at nanosecond resolution, aiming at the effect of divalent cations on the particular kinetic components of P_{680}^+ reduction. To our surprise we found only the slower, proton steered component retarded by some added cations (namely $Co^{2+}/Zn^{2+} > Fe^{2+} > Mn^{2+}$). Neither the fast component nor the apparent p*K* of the acid/base cluster around Y_Z was affected. Apparently, the divalent cations acted (electrostatically) on the proton release channel that connects the oxygen-evolving complex with the bulk water, but not on the ET between Y_Z and P_{680}^+, proper. Contrastingly, Ca^{2+} and Mg^{2+}, when added at >5 mM, *accelerated* the slow component of P_{680}^+ reduction by Y_Z and *shifted* the apparent p*K* of Y_Z from 7.4 to 6.6 and 6.7, respectively. It was evident that the binding site(s) for added Ca^{2+} and Mg^{2+} were close to Y_Z proper. The data obtained are discussed in relation to the nature of the metal-binding sites in photosystem II.

Keywords: Photosystem II; Water oxidation; Tyrosine Z; Proton coupled electron transfer; H/^{2}H isotope effect; Hydrogen bond

Abbreviations: BBY, PS II-enriched membrane fragments; BRC, bacterial reaction center; DCBQ, 2,5-dichloro-*p*-benzoquinone; DCIP, 2,6-dichlorophenolindophenol; β-DM, *n*-dodecyl-β-D-maltoside; DPC, 1,5-diphenylcarbazide; EDTA, ethylenediaminetetraacetic acid; ET, electron transfer; OEC, oxygen-evolving complex; PS II, photosystem II; P_{680}, primary donor in photosystem II; PCET, proton-controlled electron transfer; Q_A, primary electron acceptor quinone; Y_Z, Y_D, tyrosines 161 on subunits D1 and D2 of PS II

* Corresponding author. Fax: +49-541-969-2262. *E-mail address:* junge@uos.de (W. Junge).

0005-2728/01/$ – see front matter
PII: S0005-2728(01)00188-8

1. Introduction

Photosystem II (PS II) is located in thylakoid membranes of green plants and cyanobacteria. It uses the energy of light to produce molecular oxygen from water (see [1–3] for recent reviews). P_{680}, a chlorophyll (Chl) *a* moiety, is positioned at the lumenal side of the thylakoid membrane. P_{680} drives the primary charge separation, reducing the bound plastoquinones. The high midpoint potential of the oxidized species, P_{680}^{+} (about 1.15 V), drives water oxidation via intermediates. P_{680}^{+} is reduced (in tens of nanoseconds) by a tyrosine residue (D1-Tyr161, Y_Z), which is, in turn, reduced in microseconds by the oxygen-evolving complex (OEC). As cofactors, the OEC contains four manganese atoms and one atom each of Cl and of Ca. Driven by four light quanta, the OEC cycles through the increasingly oxidized states $S_0 \Rightarrow S_1 \Rightarrow S_2 \Rightarrow S_3 \Rightarrow S_4 \rightarrow S_0$. The release of dioxygen is associated with the last transition $S_4 \rightarrow S_0$, which spontaneously advances in the dark.

The core of PS II is formed by the D1 and D2 polypeptides. Their amino acid sequences resemble those of subunits L and M of the photosynthetic reaction centers of purple bacteria (BRC). The BRC crystal structures are available for *Rhodobacter sphaeroides* [4] and *Rhodopseudomonas viridis* [5] with resolutions of 2.2 Å and 2.3 Å, respectively. Electron diffraction on 2D crystals of PS II at a resolution of 8 Å [6] as well as X-ray diffraction on 3D crystals at a resolution of 3.8 Å [7] have corroborated the notion that the core of PS II resembles the one from purple bacteria except for the Mn-binding site (and the presence of cytochrome *b*-559). It has been suggested, based on the alignment of the primary structures, that Y_Z may occupy a position on subunit D1 relative to P_{680} similar to those of L-Arg135 or M-His162 in the reaction center of *Rps. viridis*.

The metal ions of PS II, Mn^{2+} and Ca^{2+}, have no counterpart in the BRC. This is why their location cannot be inferred from a sequence comparison. Mutagenesis experiments have indicated certain amino acids at the C-terminus of D1 and at the connecting loop between the A and B helices of D1 as possible ligands to Mn and Ca binding [8–10]. These data have been integrated in molecular models yielding a presumable position for the Mn cluster between Y_Z and the lumen [11]. Studies on the paramagnetic interaction between the Mn cluster and the Y_Z radical yielded conflicting results on their distance with some convergence at 8–12 Å [12–14]. The upcoming crystal structure of PS II [7] shows high electron density in a position that is compatible with the guessed one of the Mn cluster in previous modeling studies.

The Mn cluster together with the Ca atom can be eliminated from PS II by amine treatment at high pH (see e.g. [15]). The depletion is reversed under photoactivation [16–19]. Photoactivation is a complex process, which includes the following stages. (1) One Mn^{2+} ion binds to the so-called high-affinity site. It is then photooxidized to Mn^{3+}. The dissociation constant of Mn at this site is 1 μM with minor variations depending on the preparation and on the concentration of other ions in the medium. (2) The binding of a second Mn^{2+} ion is assisted by the binding of a Ca^{2+} ion ($K_d^{Ca2+} \approx 1.4$ mM). The calcium-assisted rearrangement of the protein seems to be the rate-determining step of the overall reconstitution of the Mn_4 cluster. (3) The binding of two other Mn atoms is supposed to occur promptly in the dark eventually yielding the tetra-Mn cluster. The latter forms the functional OEC together with Ca and Cl.

These data imply the existence of several metal binding sites in PS II. The one most extensively studied was the highest affinity for Mn^{2+} [20]. Fe^{2+} seems to be the only other ion which binds to this site with comparably high affinity and it is even oxidized in this position [21]. The occupation state of the high-affinity site in Mn-depleted PS II preparations has been inferred from the reduction rate of 2,6-dichlorophenolindophenol (DCIP) in the presence of 1,5-diphenylcarbazide (DPC) as an electron donor [20,22]. The binding of Mn^{2+} or, likewise, of Fe^{2+} to this site slows the rate of DCIP reduction, presumably by blocking the access of the added electron donor DPC to $(Y_Z P_{680})^{ox}$.

When PS II is depleted from Mn and Ca, the relaxation time of the reduction of P_{680}^{+} by Y_Z is retarded from nanoseconds to microseconds [23,24]. Whereas the rate of the electron transfer (ET) is practically pH-independent (in the range 5.5–8) in unperturbed and oxygen-evolving preparations, it attains a strong pH dependence after Mn depletion ranging from 0.4–1 μs at pH 9.0 to approx. 100 μs at pH 5.0. The origin of this pH dependence has been characterized [24,25]. It has been found that

one prerequisite for a rapid reduction of P_{680}^+ by Y_Z is an intact hydrogen bond system involving Y_Z and, perhaps, D1-His190. If it is disturbed either by Mn/Ca depletion or in D1-H190X mutants [25–27], the rate of P_{680}^+ reduction is kinetically steered by the probability of the deprotonation of Y_Z itself [24]. On the other hand, if the H bond system is intact, Y_Z behaves as a tyrosine anion (tyrosinate) in the reduced state and as a neutral radical in the oxidized state [28]. In Mn-depleted material the transition from a rapid to a slower reduction of the primary donor titrates with an apparent pK of about 7. This pK (pK_{Yz}^{app}) is considered a collective property of an entity involving Y_Z [24,26,27,29–31] whereas the pK of Y_Z itself when the H bond system seems to be broken ranges up to 10 [25].

In conclusion, the tyrosinate-like state of Y_Z ('Y_ZO^-') is a prerequisite for the rapid reduction of P_{680}^+. If the Y_Z-H bond entity is protonated ('Y_ZOH'), the reaction is slowed down dramatically. In the former case the reaction is a mere electron transfer, in the latter the electron transfer is steered by the deprotonation of 'Y_ZOH' (proton-controlled electron transport (PCET); see [32]).

Experimental evidence for the tyrosinate-like properties of Y_Z at pH $\approx$ 9 but not at pH $\approx$ 6 in the Mn-depleted PS II preparations was obtained from Y_Z^{ox}/Y_Z FTIR difference spectra [33]. The difference spectra of Y_Z^{ox}/Y_Z in oxygen-evolving and Mn-depleted PS II core particles were re-examined as a function of the pH [28], again leading to the suggestion that a hydrogen-bonded tyrosinate is oxidized to a hydrogen-bonded tyrosine radical at pH >7 without release of the shared proton into the bulk medium, whereas at pH <7 in the Mn-depleted preparations a neutral tyrosine is much more slowly oxidized to a neutral tyrosine radical after the release of a proton into the bulk medium. For further discussion on the anionic nature of Y_Z see also [34–37].

In Mn-depleted preparations, the addition of Mn^{2+} and some other divalent cations (Co, Ni, Cu, Zn) slows down the overall rate of P_{680}^+ reduction [38] (at pH 7.4–7.5) [39]. The apparent binding constant is approx. 50 μM for Mn^{2+} [38]. The slowing has been attributed to the binding of a cation in the direct vicinity of Y_Z, which by electrostatic influence increases the midpoint potential of Y_Z and thereby decreases the free energy difference ΔG of the ET from Y_Z to P_{680}^+ [38,39]. In the latter articles it has not been noted, because of low time resolution, that the kinetics of P_{680}^+ is multiphasic at neutral pH with at least two components with rate constants k_f and k_s (see above). This prompted us to reinvestigate the effects of added divalent cations of Mn, Fe, Mg and Ca on two kinetic components of the reduction of P_{680}^+ by Y_Z, the ET and PCET.

2. Materials and methods

2.1. Oxygen-evolving PS II core particles

Oxygen-evolving PS II core particles were prepared from pea seedlings according to van Leeuwen and co-workers [40] with certain modifications [41] and stored at −80°C in 20 mM Bis-Tris–HCl, 400 mM sucrose 20 mM $MgCl_2$, 5 mM $CaCl_2$, 10 mM $MgSO_4$, 0.03% (w/v) *n*-dodecyl-β-D-maltoside (β-DM) at pH 6.3. The rate of oxygen evolution under saturating continuous light determined with 0.5 mM 2,5-dichloro-*p*-benzoquinone (DCBQ) as artificial electron acceptor was around 1000–1300 μmol/mg (Chl)/h.

2.2. Mn depletion

Mn depletion of the OEC of PS II core particles was achieved as follows: Tris buffer (0.8 M, pH 8.8) was added to stock of PS II core particles (concentration around 500 μM Chl) in the ratio 29:1 (v/v) to sediment Mn-depleted PS II particles by centrifugation. The samples were incubated 15 min under room light and temperature, then they were pelleted, washed and suspended in buffer A (sucrose 0.4 M, NaCl 15 mM, MES–NaOH 50 mM, pH 6.2). The rest of oxygen-evolving activity was less then 5%.

2.3. Electron transport activity

Electron transport activity in the Mn-depleted PS II particles from DPC to DCIP was measured spectrophotometrically at 600 nm in buffer A containing 10 μM Chl, 200 μM DPC and 40 μM DCIP. An extinction coefficient of 21.8 mM^{-1} cm^{-1} was used for the deprotonated form of DCIP [42] to calculate the rates of photoreduction of DCIP. Freshly pre-

pared stock solutions of DPC, DCIP, $MnCl_2$, $ZnCl_2$, $CoCl_2$ and $FeSO_4$ were used. $FeCl_3$ was prepared as a stable complex of ferric iron with sucrose as described in [43].

2.4. ^2H_2O substitution

^2H_2O was substituted for H_2O as follows: after thawing, the PS II-containing material was suspended in a medium with ^2H_2O (99.7% pure), at p*L* 6.2 (L: lyonium ion, H or ^2H) and at the final chlorophyll concentrations for the measurements. Samples were then incubated in the light (approx. 1 mW cm^{-2}) for 5 min at room temperature and dark-adapted for 15 min prior to the first flash train. The maximum H/^{2}H isotope effects were already observed after shorter incubation time, e.g. after less than 1 min, as apparent from measurements of absorption changes at 827 nm as a function of the incubation interval (data not documented).

2.5. Reduction of P^+_{680}

The reduction of P^+_{680} was measured by flash-induced absorption changes at 827 nm as described in [24] with the following modifications: in some experiments a Q-switched, frequency-doubled Nd:YAG laser (infinity, coherent) served as excitation source (flash duration 2 ns, 532 nm). The electrical bandwidth of the system was up to 150 MHz (dwell time 4 ns). Transients were digitized and averaged for signal-to-noise improvement on a Tektronix DSA602 digital oscilloscope. Samples contained 50 μM chlorophyll, and 0.5 mM DCBQ as electron acceptor. For pH-dependent experiments, we used buffers as described in [24], but we avoided the use of Bis-Tris buffer together with calcium ions, because we observed a chelator effect that decreased the pH stability of the sample.

3. Results

3.1. Probing sites with affinity for Mn^{2+} and Fe^{2+}

Previous studies on the effect of divalent cations on the reduction of P^+_{680} by Y_Z were carried out on Mn-depleted PS II-enriched membrane fragments (BBY) [38]. In this work we used PS II core complexes.

3.1.1. DPC/DCIP test

The intactness of the high-affinity Mn-binding site was monitored by the reduction of DCIP with DPC as electron donor. As given in Table 1 the maximum rate of DCIP reduction was 156 μmol/mg (Chl)/h. This rate was about halved upon addition of Mn^{2+} or Fe^{2+} at 5 μM, conforming to previous reports on BBY membranes [22,44].

We found that this behavior was independent of the detergent concentration tested up to 0.03% β-DM. When the sample was incubated with Mn^{2+}, then illuminated and thereafter washed to remove unbound Mn^{2+}, the inhibition was reversed. Such reversibility was not observed with Fe^{2+}. Apparently, the quantum yield of the photooxidation of Fe^{2+} was larger than that of the photooxidation of Mn^{2+}.

3.1.2. Kinetics of P^+_{680} reduction

In Mn-depleted core particles the reduction of P^+_{680} by Y_Z proceeds with two kinetic phases with relaxation times of about 1 μs and 10–100 μs, respectively [24]. Absorption transients of P^+_{680} were monitored at 820 nm with a time resolution of 50 ns per address of the signal averager. The aim was to resolve any influence of the addition of Mn^{2+} and Fe^{2+} on these two phases. In agreement with previous observations [38,39] we found no marked change in the kinetics in response to the addition of Mn^{2+} or Fe^{2+} cations at <10 μM (see Fig. 1A and 3).

Table 1
DCIP photoreduction with DPC as electron donor: effects of Mn^{2+}/Fe^{2+} on its rate

Addition	DCIP photoreduction (μmol/mg (Chl)/h), relative yield is given in parentheses
(Control)	156 (100%)
5 μM $MnCl_2$	83 (53%)
5 μM $FeSO_4$	73 (47%)
5 μM $FeSO_4$, 0.03% β-DM	72 (46%)
5 μM $MnCl_2$ plus centrifugation[a]	150 (96%)
5 μM $FeSO_4$ plus centrifugation[a]	100 (64%)

[a]5 min incubation in the presence of Mn^{2+}/Fe^{2+} at room light followed by centrifugation to remove the unbound cations.

Fig. 1B shows that the addition of Mn^{2+} at a 'moderate' concentration of 50 μM to the Mn-depleted PS II core particles at pH 7.4 (dissolved in 30% glycerol) increased the half-decay time of the slow component of P^+_{680} reduction from 9 to 17 μs. The fast decay, however, was unaffected (0.85 and 0.95 μs (±0.1 μs), respectively). The relative extents of both phases were not affected either. In the light of previous work [24], the latter implied that the pK^{app}_{Yz} was not affected (*vide infra* for details). In the absence of glycerol in the buffer, the half-time increase was smaller, i.e. from 9 to 12 μs. As expected, the slowing of the P^+_{680} reduction in response to Mn^{2+} addition was more pronounced at acidic pH values (Fig. 1A, pH 6.2), where the contribution of the slow kinetic phase (k_s) was larger.

In agreement with the previous data [38,39] we observed that divalent cations acted in an affinity series $Co^{2+}/Zn^{2+} > Fe^{2+} > Mn^{2+}$.

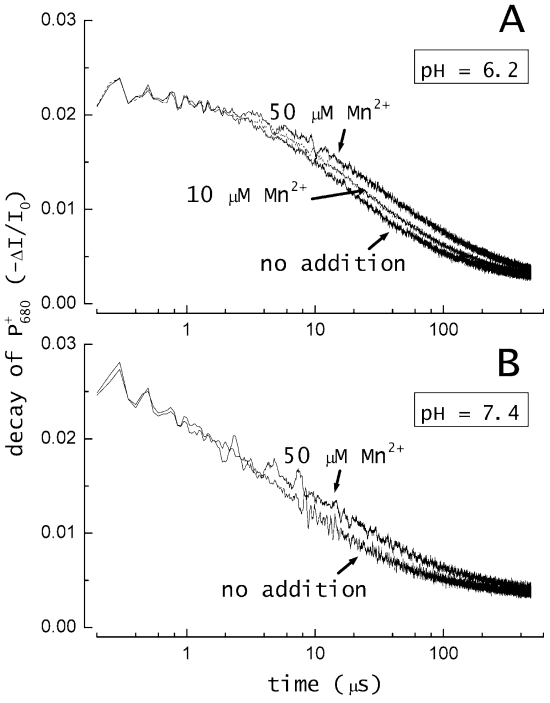

Fig. 1. Reduction of P^+_{680} as function of time, monitored by flash-induced absorption spectroscopy at 827 nm – effect of Mn^{2+}. (A) pH 6.2, control data and with 10 and 50 μM $MnCl_2$ added; (B) pH 7.4, control data and with 50 μM $MnCl_2$ added. Conditions: Mn-depleted core particles (50 μM Chl), the medium contained buffer A (0.4 M sucrose, 15 mM NaCl, 50 mM MES–HEPES buffer at pH 6.2/7.4, respectively), 30% (v/v) glycerol, 0.03% (w/v) β-DM, 0.5 mM DCBQ. The time resolution was 50 ns per address; 30 transients were averaged for each trace (with a flash separation of 5 s).

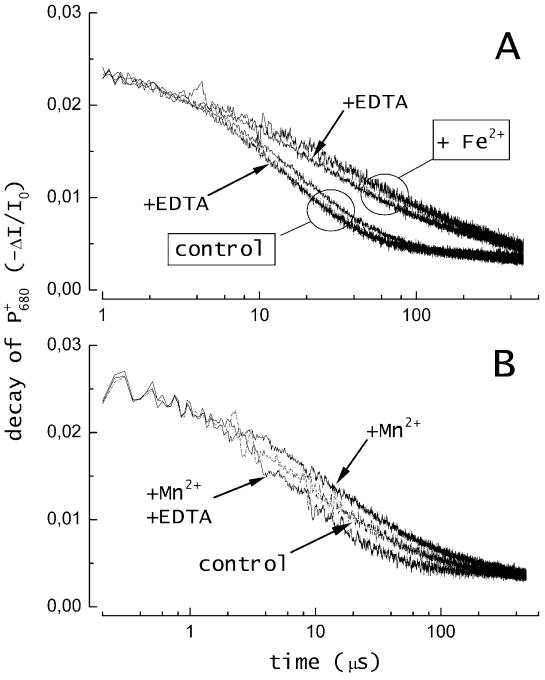

Fig. 2. Irreversibility of cation-binding – effect of added EDTA on P^+_{680} reduction kinetics influenced by:
(A) Fe^{2+} (10 μM $FeSO_4$, 20 μM EDTA, pH 6.2, other conditions as in Fig. 1, but without glycerol), (B) Mn^{2+} (50 μM $MnCl_2$, 100 μM EDTA, pH 7.4, other conditions as in Fig. 1).

As noted in Section 1, Fe^{2+} is the only other divalent cation besides Mn^{2+} that tightly binds to the high-affinity site. Fig. 2A shows data on the reversibility of the binding of Fe^{2+} and Mn^{2+} as revealed by the P_{680} kinetics. The addition of 20 μM ethylenediaminetetraacetic acid (EDTA) to the control sample led to the marginal acceleration of the P^+_{680} reduction, due to the scavenging of some residual divalent cations. A similarly small acceleration was observed when EDTA was added to a sample containing 10 μM Fe^{2+}. The addition of EDTA upon 50 μM $MnCl_2$ caused, however, a marked acceleration of the P^+_{680} reduction. This observation allowed the conclusion that the iron cation in the 'moderate-affinity site' was irreversibly bound, in contrast to Mn^{2+} (see Fig. 2B). One possible explanation for this 'irreversible' binding could be the prompt oxidation of the iron cation by Y_Z (see Section 4 for further details).

The irreversible Fe^{2+} binding is instrumental as it avoids ambiguity on the comparison of inhibition data obtained under the steady state conditions with those measured in a single turnover mode (DPC/DCIP test and P^+_{680} reduction, respectively).

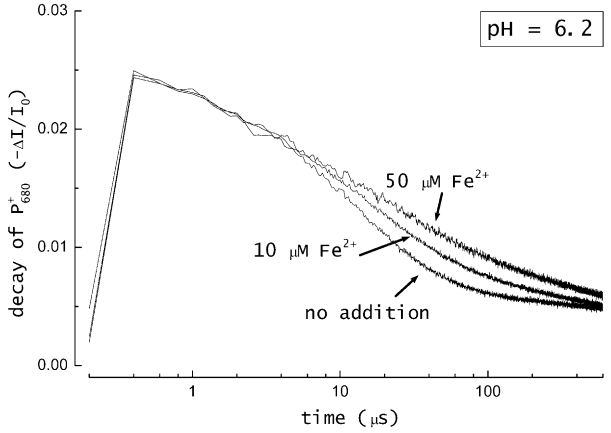

Fig. 3. The reduction of P_{680}^+ – concentration effect of Fe^{2+}. Control sample and with 10/50 μM $FeSO_4$ added, respectively. 50 and 500 μM $FeSO_4$ (data not shown) gave almost the same curve. Conditions as in Fig. 1, but without glycerol, pH 6.2. The dwell time of the digital oscilloscope was 200 ns.

We studied the effects of Fe^{2+} on the kinetics of P_{680}^+ reduction in more detail. The half-decay time of the slow phase of P_{680}^+ reduction increased from 13 μs to 27 μs upon the addition of Fe^{2+} at pH 6.2 (Fig. 3). The concentration dependence (data with 10, 50 and 500 μM $FeSO_4$ added) revealed a dissociation constant K_d of about 10 μM.

Fig. 4 shows the effect of substitution of H_2O for ^2H_2O. In accordance with our previous report [24], only the slow phase was significantly retarded by ^2H_2O. The effects of Fe^{2+} and of the isotope substitution were additive.

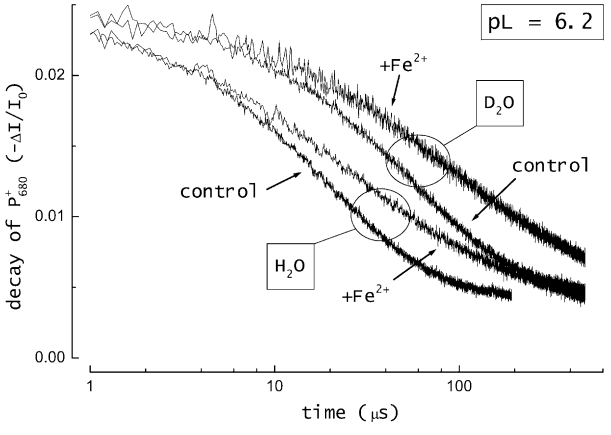

Fig. 4. Comparison of P_{680}^+ reduction kinetics influenced by Fe^{2+} (50 μM $FeSO_4$) in H_2O and ^2H_2O at pL 6.2. Conditions as in Fig. 3.

3.2. Influence of Ca^{2+} and Mg^{2+} on P_{680}^+ reduction in Mn-depleted PS II particles

The addition of high concentrations of Ca^{2+} *accelerated* the overall reduction rate of P_{680}^+ with an apparent K_d of about 10 mM (Fig. 5). These ions are considered chaotropic reagents ('structure breakers'); at concentrations of 100 mM they damaged PS II at the acceptor side in 15–20% of the complexes, as evident from an additionally kinetic component of P_{680}^+ reduction that was faster than 10 ns. This component could be ascribed to the recombination of pheophytin with P_{680}. Still it seemed that the kinetic features of the observed electron transfer between Y_Z and P_{680}, i.e. for the residual part of the data, were not disturbed. In Fig. 5A the kinetic traces measured at pH 5.5 are shown. In the absence of Ca^{2+}, only the slow component k_s is present. Addition of Ca^{2+} led to an acceleration of k_s and, simultaneously, to a turning up of the fast component k_f that manifested itself, at low time resolution, in a decrease in the

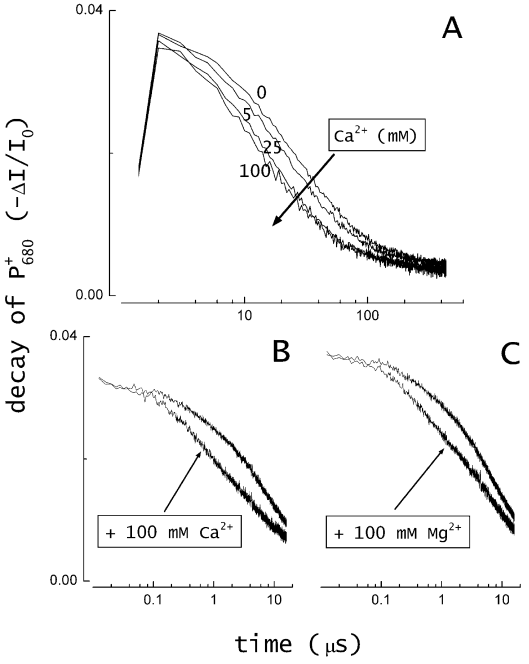

Fig. 5. Influence of Ca^{2+} and Mg^{2+} on the reduction kinetics of P_{680}^+.
(A) 5, 25 and 100 mM $CaCl_2$, respectively, were added. pH 5.5, MES was used as pH buffer, dwell time was 1 μs.
(B,C) 100 mM $CaCl_2$/$MgCl_2$ were added, respectively. pH 7.0, HEPES was used as pH buffer, dwell time was 4 ns. Other conditions as in Fig. 3.

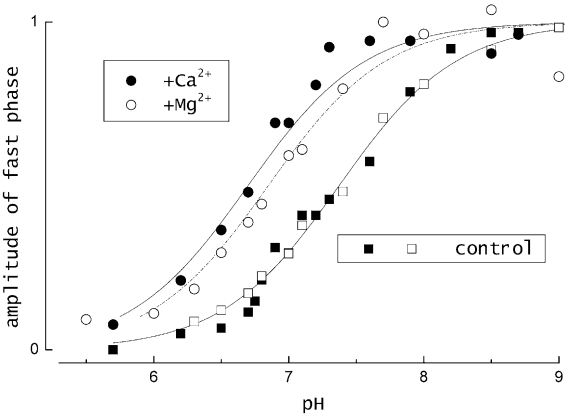

Fig. 6. The relative contribution of the fast phase k_f of the P^+_{680} reduction kinetics as function of the medium pH (■,□) control measurements; (●) 100 mM $CaCl_2$; (○) 100 mM $MgCl_2$; (—) fitted titration curve (see text and Table 2 for details). Experimental conditions were the same as in Fig. 5B,C.

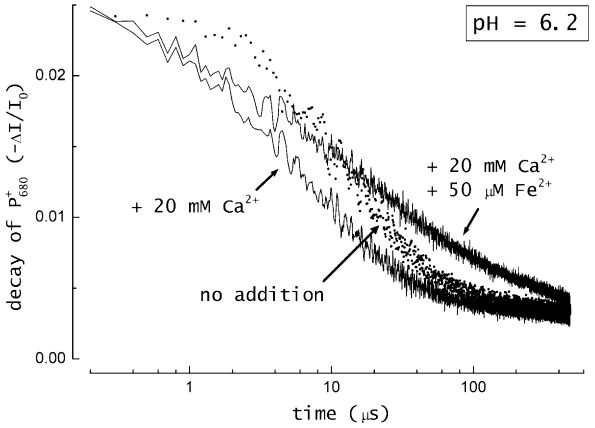

Fig. 7. Influence of the simultaneous addition of Fe^{2+} and Ca^{2+} on the reduction of P^+_{680}. Conditions were as in Fig. 3.

apparent signal amplitude. The parallel measurements at higher time resolution allowed resolving the component k_f that appeared at pH 5.5 in the presence of Ca^{2+} (not documented). The relative contribution of this newly emerging fast phase was small, only 5–10% at this pH. The latter data were used for the normalization of the overall amplitudes of the P^+_{680} kinetic traces in Fig. 5A. The initial extents of the transients at 820 nm were then independent of the concentration of added Ca^{2+}. The concentration dependence of the Ca^{2+} effects revealed a K_m around 10 mM. Similar effects were observed upon addition of Mg^{2+}, although the acceleration of the slower kinetic component k_s was less pronounced (not shown). Both ions affected a change in *contributions* of the slow and fast components as manifested by the appearance of the fast component at low pH. At neutral pH the decrease of the slower component k_s for the benefit of the faster one (k_f) was more pronounced (see Fig. 5B and C for Ca^{2+} and Mg^{2+} effects, respectively).

The kinetic analysis of data (as shortly described above, see also [24] for the procedure) indicated a shift of the apparent pK^{app}_{Yz} value from 7.4 to 6.7 (6.8) in response to the addition of 100 mM Ca^{2+} (or Mg^{2+}) (see Fig. 6).

When 50 μM Fe^{2+} was added on top of 20 mM Ca^{2+}, the characteristic effects of both cations were observed simultaneously: k_s slowed down and the ratio between the amplitudes of the two kinetic components (with rates k_f and k_s) changed, indicating the shift of the apparent pK (Fig. 7). We considered this as an indication that Ca^{2+} and Fe^{2+} were bound independently from each other and to different sites.

Table 2 contains an overview of the numerical results describing the kinetics of P^+_{680} reduction by Y_Z in terms of k_f, k_s, and pK^{app}_{Yz}.

4. Discussion

Manganese and calcium are essential ionic cofactors of photosynthetic water oxidation. There are several binding sites for divalent cations at the donor side of photosystem II. They have been previously

Table 2
Parameters of P^+_{680} reduction kinetics (monitored by flash-induced absorption spectroscopy at 827 nm)

Addition	(Control)			50 μM $MnCl_2$		50 μM $FeSO_4$		100 mM $CaCl_2$	100 mM $MgCl_2$
Medium pH	5.5	6.2	7.4	6.2	7.4	6.2	7.4	5.5	5.5
Half-rise time of the slow phase k_s (in μs, rel. S.D. ≤5%)	27	13	9	20[a]	12 (17[a])	27	12	18	23
pK^{app}_{Yz} (S.D. 0.1)					7.3			6.6	6.7

[a]In the presence of 30% glycerol.

studied mainly in Mn- (and Ca-) depleted material both in PS II-enriched membranes and in PS II core particles ([38,39]; see Section 1 for other references). In previous studies the time resolution was too low to clearly resolve the rapid components of the ET at the donor side of PS II. In this work we resumed this topic with emphasis on nanosecond time resolution of the electron transfer between the primary, P_{680}, and the secondary electron donor in PS II, Y_Z. The goal was to discriminate between two modes of the respective ET in Mn-depleted PS II, namely a fast mode of ET ($\lesssim$1 μs) and a slower one of PCET (10–100 μs) [24–26, 31]. The protonation state of a functionally important hydrogen-bonded cluster around Y_Z determines the relative extents of these two phases. It titrates with a pK around 7 in the Mn-depleted preparations. Several authors have emphasized the importance of an anionic or partially anionic nature of Y_Z for its functioning in efficient PS II [24,28,34–37]. The predominance of the fast mode of ET from Y_Z to P_{680}^+ at alkaline pH is believed to be either caused by the absence of the phenolic proton of Y_Z (see e.g. [34]) or due to the susceptibility of the hydrogen-bonded cluster for this proton (see e.g. [45]). At acid pH, the slow phase dominates because the electron transfer requires the transfer of the Y_Z proton away into the aqueous phase before it can proceed (see [24]). This interpretation views the PCET as a consecutive proton/electron reaction. We attempted to elucidate the role of the binding of divalent cations on the ET proper on the one hand, and on the controlling proton transfer on the other.

We found no effect on the rate of the electron transfer between Y_Z and P_{680} by the binding of Mn or Fe (added at <10 μM) to the *high-affinity site*, although the occupancy of this site was clearly apparent by the standard test, namely, measuring under continuous light the rate of the ET between the donor/acceptor couple DPC/DCIP. This result concerned both kinetic modes, ET and PCET. As a consequence this site neither controlled the proton outlet channel from Y_Z into the aqueous bulk, nor, by electrostatic interaction, the ET itself. There were two options for the latter, either the high-affinity site was located right at the protein–water interface and thereby electrostatically screened, or the binding of the divalent cations expelled the exactly equivalent number of protons or other univalent ions from this site, thereby electrostatically silencing this transition. The latter phenomenon has been addressed experimentally; it has been observed that *only one* proton is released upon binding of one Mn^{2+} atom [46]. Accordingly, the location of the high-affinity site at the protein–water interface seems to be more probable.

When Mn, Fe or other divalent cations were added at higher concentrations (>10 μM) to bind to the *moderate-affinity site*, the overall rate (measured with low time resolution) of the ET from Y_Z to P_{680}^+ was retarded in the sequence Co/Zn > Fe > Mn as previously found [38,39]. Closer inspection showed that the rate of the fast phase was not affected at all, whereas the slow phase was retarded.

The slowing of P_{680}^+ reduction by the binding of divalent cations to the moderate-affinity site has been attributed previously to the electrostatic influence of the bound cation on the free energy gap between Y_Z and P_{680}^+. It has been speculated that binding of a cation closer to Y_Z than to P_{680}^+ could increase the redox potential of the former. Based on this interpretation, the moderate-affinity site has been assumed to be in the vicinity of Y_Z [38,39]. This does not seem to be the case. The occupancy of the moderate-affinity site by positively charged divalent cations does neither affect k_f (ET from Y_Z to P_{680}^+ [24]) nor pK_{Yz}^{app}. The latter value has been shown to be sensitive to environmental changes [24,47]; it actually decreases in the presence of Ca^{2+} and Mg^{2+} (see below). We argued elsewhere [24] that the slower component of the P_{680}^+ reduction is kinetically steered by the deprotonation of Y_Z, which is a prerequisite for its oxidation to the neutral tyrosine radical (see Section 1). In line with this argument, we found the slow reduction of P_{680}^+ to be weakly pH-dependent in a way suggesting the influence of the surface potential at the lumenal side of PS II on the energy profile of proton release [24]. It is conceivable that the slowing of k_s in response to the binding of cations may reflect the location of the moderate-affinity binding site close to the respective proton outlet, between Y_Z and the lumenal side of core particles.

Our data in Fig. 6 show that the binding of Ca^{2+} (Mg^{2+}) when added at >10 mM caused a decrease in pK_{Yz}^{app} by 0.7 (0.6) pH units. A similar shift (0.5–

0.6 pH units) of pK_{Yz} has been observed in the *Synechocystis* sp. PCC 6803 core PS II particles in response to addition of 20 mM Ca^{2+} and 5 mM Mg^{2+} [25]. It is conceivable that Ca^{2+} (Mg^{2+}) binds to the components of the native Ca^{2+}-binding site. The latter is believed to be close to the Mn cluster [9,10,48]. In fully competent Mn-containing core particles, the Ca atom can be selectively extracted by acid treatment, without damaging the Mn cluster. The extraction might be owed to the protonation of carboxy groups, which serve as Ca^{2+} ligands. Such a Ca^{2+} extraction shifts, in a reversible way, the pK_{Yz}^{app} from <5.0 to approx. 7.0 [47]. The same neutral pK_{Yz}^{app} is observed in the absence of both Ca^{2+} and the Mn cluster [24]. This indicates that the electrostatic/structural influence of Ca^{2+} is more important in defining the pK_{Yz}^{app} value than the one of the Mn cluster. In the absence of the Mn cluster as in our experiments, the reconstitution of the native Ca-binding site could hardly be complete. We observed the same acidic direction of the shift in pK_{Yz}^{app} upon the addition of Ca^{2+} as in the presence of the Mn cluster. The smaller magnitude of the Ca^{2+}-induced pK_{Yz}^{app} shift in the absence of the Mn cluster is tentatively attributed to the distortion of the binding site.

4.1. Outlook

It is attractive to tentatively locate the three metal-binding sites in PS II relative to Y_Z in the light of the structural homology of PS II with the bacterial RC. The most recent structure of *Rps. viridis* RC with a resolution of 2.3 Å [5] shows that both L-Arg135 and M-His162, the counterparts of Y_Z in the primary structure, form hydrogen-bonded clusters with nearby charged residues and that these clusters are connected with the lumenal surface of protein by water-filled channels. It is attractive to speculate that the water-filled cavities that are seen in the crystal structure of the RC might be related to a cavity that is believed to connect Y_Z and the Mn cluster with the lumen. Such a cavity is needed to deliver water molecules to the place of their cleavage in PS II and to remove the released protons. The cavity is likely involved in the assembly of the Mn cluster. The latter process includes the transfer of four Mn atoms from the lumen to the protein. The high-affinity site with its very low dissociation constant (approx. 100 nM in native membranes) may serve as a trap for the Mn^{2+} cations. This site is expected to lie at the water boundary, away from Y_Z. Correspondingly, it is not surprising that Mn^{2+} binding to this site is without any influence on the kinetics of reduction of P_{680}^+ by Y_Z (see [38,39] and this work). At the next stage the second Mn cation is bound and oxidized. The binding site of the Mn dimer might be closer to the proton release channel, which connects Y_Z with the water boundary and could account for the 'moderate-affinity' Mn-binding site. The Ca^{2+}-assisted assembly of the Mn cluster is coupled with a conformational change, which implies a certain mobility of the involved protein domains. With the functional Mn cluster assembled, the Ca atom may stiffen the structure, carrying a gate-keeping function as discussed in [49]. The acidic shift in pK_{Yz}^{app} that we observed in response to the Ca^{2+} addition might indicate that some affinity to Ca^{2+} is retained even in the absence of the Mn cluster.

A common feature of both Mn-binding sites explored in this study was the irreversibility of Fe^{2+} compared to Mn^{2+} binding (see Table 1 and Fig. 2). It was interpreted to indicate a higher quantum yield of Fe^{2+} oxidation as compared with those of Mn^{2+} oxidation which is rather low [16]. This might be due to the lower redox potential of the Fe^{2+}/Fe^{3+} redox pair compared with the Mn^{2+}/Mn^{3+} redox couple. The redox potential of the Mn^{2+}/Mn^{3+} redox pair is 1.51 V. That is too high for the direct oxidation by Y_Z ($E_m \approx 1$ V). Therefore it is believed than Mn^{2+} is oxidized to Mn^{3+} after the redox potential of the Mn^{2+}/Mn^{3+} redox couple is decreased due to the coordination of the Mn atom by the protein ligands. The E_m of the Fe^{2+}/Fe^{3+} redox pair is lower, 0.77 V; hence in this case the oxidation of Fe^{2+} may promote its binding and make it irreversible.

To check how the binding of Mn atoms to their final positions in the functional OEC influences the rate of Y_Z oxidation, one has to follow the latter reaction under conditions of photoactivation. This is an interesting perspective for further studies.

Acknowledgements

The authors thank Hella Kenneweg for excellent technical assistance and Drs. Monika Hundelt and

Michael Haumann for helpful discussions. We also thank Prof. Charles Dismukes for a useful advice. Financial support from the Deutsche Forschungsgemeinschaft (SFB 431/D8, Mu-1285, Ju-13/97), the Fonds der Chemischen Industrie, and INTAS (INTAS-93-2852) is gratefully acknowledged.

References

[1] B.A. Diner, G.T. Babcock, in: D.R. Ort, C.F. Yocum (Eds.), Structure, Dynamics, and Energy Conversion Efficiency in Photosystem II, vol. 4, Kluwer Academic Publishers, Dordrecht, 1996, pp. 213–247.
[2] M. Haumann, W. Junge, Biochim. Biophys. Acta 1411 (1999) 86–91.
[3] A.Y. Mulkidjanian, Biochim. Biophys. Acta 1410 (1999) 1–6.
[4] M.H. Stowell, T.M. McPhillips, D.C. Rees, S.M. Soltis, E. Abresch, G. Feher, Science 276 (1997) 812–816.
[5] J. Deisenhofer, I. Sinning, H. Michel, J. Mol. Biol. 246 (1995) 429–457.
[6] K.H. Rhee, E.P. Morris, J. Barber, W. Kühlbrandt, Nature 396 (1998) 283–286.
[7] A. Zouni, H.T. Witt, J. Kern, P. Fromme, N. Krauss, W. Saenger, P. Orth, Nature 409 (2001) 739–743.
[8] H.B. Pakrasi, W.F.J. Vermaas, in: J. Barber (Ed.), Protein Engineering of Photosystem II, Kluwer Academic Publishers, Dordrecht, 1992, pp. 231–257.
[9] H.A. Chu, A.P. Nguyen, R.J. Debus, Biochemistry 34 (1995) 5859–5882.
[10] H.A. Chu, A.P. Nguyen, R.J. Debus, Biochemistry 34 (1995) 5839–5858.
[11] B. Svensson, C. Etchebest, P. Tuffery, P. van Kan, J. Smith, S. Styring, Biochemistry 35 (1996) 14486–14502.
[12] P. Dorlet, M.D. Valentin, G.T. Babcock, J. Phys. Chem. B 102 (1998) 8239–8247.
[13] J.M. Peloquin, K.A. Campbell, R.D. Britt, J. Am. Chem. Soc. 120 (1998) 6840–6841.
[14] K.V. Lakshmi, S.S. Eaton, G.R. Eaton, H.A. Frank, G.W. Brudvig, J. Phys. Chem. B 102 (1998) 8327–8335.
[15] J. Cole, M. Boska, N.V. Blough, K. Sauer, Biochim. Biophys. Acta 848 (1986) 41–47.
[16] L. Zaltsman, G.M. Ananyev, E. Bruntrager, G.C. Dismukes, Biochemistry 36 (1997) 8914–8922.
[17] N. Tamura, G. Cheniae, Biochim. Biophys. Acta 890 (1987) 179–194.
[18] N. Tamura, Y. Inoue, G.M. Cheniae, Biochim. Biophys. Acta 976 (1989) 173–181.
[19] A.F. Miller, G.W. Brudvig, Biochemistry 29 (1990) 1385–1392.
[20] B.D. Hsu, J.Y. Lee, R.L. Pan, Biochim. Biophys. Acta 890 (1987) 89–96.
[21] B.K. Semin, I.I. Ivanov, A.B. Rubin, F. Parak, FEBS Lett. 375 (1995) 223–226.
[22] C. Preston, M. Seibert, Biochemistry 30 (1991) 9615–9624.
[23] H. Conjeaud, P. Mathis, Biochim. Biophys. Acta 590 (1980) 353–359.
[24] R. Ahlbrink, M. Haumann, D. Cherepanov, O. Bögershausen, A. Mulkidjanian, W. Junge, Biochemistry 37 (1998) 1131–1142.
[25] A.M. Hays, I.R. Vassiliev, J.H. Golbeck, R.J. Debus, Biochemistry 38 (1999) 11851–11865.
[26] A.M. Hays, I.R. Vassiliev, J.H. Golbeck, R.J. Debus, Biochemistry 37 (1998) 11352–11365.
[27] F. Mamedov, R.T. Sayre, S. Styring, Biochemistry 37 (1998) 14245–14256.
[28] M. Haumann, A. Mulkidjanian, W. Junge, Biochemistry 38 (1999) 1258–1267.
[29] K. Shigemori, H. Mino, A. Kawamori, Plant Cell Physiol. 38 (1997) 1007–1011.
[30] F. Rappaport, J. Lavergne, Biochemistry 36 (1997) 15294–15302.
[31] B.A. Diner, D.A. Force, D.W. Randall, R.D. Britt, Biochemistry 37 (1998) 17931–17943.
[32] R.I. Cukier, D.G. Nocera, Annu. Rev. Phys. Chem. 49 (1998) 337–369.
[33] C. Berthomieu, R. Hienerwadel, A. Boussac, J. Breton, B.A. Diner, Biochemistry 37 (1998) 10547–10554.
[34] A.Y. Mulkidjanian, FEBS Lett. 463 (1999) 199–204.
[35] J.H. Nugent, A.M. Rich, M.C. Evans, Biochim. Biophys. Acta 1503 (2001) 138–146.
[36] F. Rappaport, J. Lavergne, Biochim. Biophys. Acta 1503 (2001) 246–259.
[37] B.A. Diner, Biochim. Biophys. Acta 1503 (2001) 147–163.
[38] C.W. Hoganson, P.A. Casey, O. Hansson, Biochim. Biophys. Acta 1057 (1991) 399–406.
[39] A. Magnuson, L.E. Andreasson, Biochemistry 36 (1997) 3254–3261.
[40] P.J. van Leeuwen, M.C. Nieveen, E.J. van de Meent, J.P. Dekker, H.J. van Gorkom, Photosynth. Res. 28 (1991) 149–153.
[41] O. Bögershausen, W. Junge, Biochim. Biophys. Acta 1230 (1995) 177–185.
[42] J.M. Armstrong, Biochim. Biophys. Acta 86 (1964) 194–197.
[43] P.J. Charley, B. Sarkar, C.F. Stitt, P. Saltman, Biochim. Biophys. Acta 69 (1963) 313–321.
[44] D.J. Blubaugh, G.M. Cheniae, in: N. Murata (Ed.), Photoassembly of the Photosystem II Manganese Cluster, Kluwer Academic Publishers, Dordrecht, 1992, pp. 361–364.
[45] M.J. Schilstra, F. Rappaport, J.H.A. Nugent, C.J. Barnett, D.R. Klug, Biochemistry 37 (1998) 3974–3981.
[46] G.M. Ananyev, L. Zaltsman, C. Vasko, G.C. Dismukes, Biochim. Biophys. Acta 1503 (2001) 52–68.
[47] M. Haumann, W. Junge, Biochim. Biophys. Acta 1411 (1999) 121–133.
[48] P.J. Nixon, B.A. Diner, Biochemistry 31 (1992) 942–948.
[49] J. Tso, M. Sivaraja, G.C. Dismukes, Biochemistry 30 (1991) 4734–4739.